

# Coupling Assembly of the E-Cadherin/ $\beta$ -Catenin Complex to Efficient Endoplasmic Reticulum Exit and Basal-lateral Membrane Targeting of E-Cadherin in Polarized MDCK Cells

Yih-Tai Chen, Daniel B. Stewart, and W. James Nelson

Department of Molecular and Cellular Physiology, Stanford University School of Medicine, Stanford, California 94305-5435

**Abstract.** The E-cadherin/catenin complex regulates  $\text{Ca}^{++}$ -dependent cell–cell adhesion and is localized to the basal-lateral membrane of polarized epithelial cells. Little is known about mechanisms of complex assembly or intracellular trafficking, or how these processes might ultimately regulate adhesion functions of the complex at the cell surface. The cytoplasmic domain of E-cadherin contains two putative basal-lateral sorting motifs, which are homologous to sorting signals in the low density lipoprotein receptor, but an alanine scan across tyrosine residues in these motifs did not affect the fidelity of newly synthesized E-cadherin delivery to the basal-lateral membrane of MDCK cells. Nevertheless, sorting signals are located in the cytoplasmic domain since a chimeric protein (GP2CAD1), comprising the extracellular domain of GP2 (an apical membrane protein) and the transmembrane and cytoplasmic domains of E-cadherin, was efficiently and specifically delivered to the basal-lateral membrane. Systematic dele-

tion and recombination of specific regions of the cytoplasmic domain of GP2CAD1 resulted in delivery of <10% of these newly synthesized proteins to both apical and basal-lateral membrane domains. Significantly, >90% of each mutant protein was retained in the ER. None of these mutants formed a strong interaction with  $\beta$ -catenin, which normally occurs shortly after E-cadherin synthesis. In addition, a simple deletion mutation of E-cadherin that lacks  $\beta$ -catenin binding is also localized intracellularly. Thus,  $\beta$ -catenin binding to the whole cytoplasmic domain of E-cadherin correlates with efficient and targeted delivery of E-cadherin to the lateral plasma membrane. In this capacity, we suggest that  $\beta$ -catenin acts as a chauffeur, to facilitate transport of E-cadherin out of the ER and the plasma membrane.

**Key words:** polarity • epithelia • adhesion • protein targeting • membrane domains

**E**PITHELIAL cells form barriers that separate the internal milieu from the outer environment of multicellular organisms, and vectorially transport ions and solutes between these compartments. To perform these functions, these cells form cell–cell contacts through cadherin adhesion proteins, establish tight seals between cell–cell contacts (tight junctions), and organize the plasma membrane into structurally and functionally distinct domains, termed apical and basal-lateral, that face these different compartments (Rodriguez-Boulan and Nelson, 1989).

Localization of transmembrane proteins to specific plasma membrane domains is achieved by protein sorting in the Golgi and subsequent delivery to specific membrane

domains, and by selective retention of proteins in the plasma membrane (Nelson, 1992). Molecular mechanisms involved in protein sorting and delivery are poorly understood. To date, the only identified sorting signal for apical membrane proteins in MDCK cells is a glycosylphosphatidylinositol (GPI)<sup>1</sup> linkage (Brown et al., 1989; Lisanti et al., 1989; for a recent review, see Nosjean et al., 1997). How the lipid anchor specifies apical domain-specific sorting and targeting in the TGN is not clear. It has been proposed that the GPI anchor enables the protein to enter glycosphingolipid clusters and, thereby, to be sorted to the apical membrane domain (Simons and Wandinger, 1990; Weimbs et al., 1997).

Several amino acid motifs have been identified that specify type-I transmembrane protein sorting in the TGN and delivery to the basal-lateral membrane (Rodriguez-

Address correspondence to W. James Nelson, Department of Molecular and Cellular Physiology, Stanford University School of Medicine, Stanford, CA 94305-5435. Tel.: (650) 725-7596. Fax: (650) 498-5286. E-mail: wjnelson@leland.stanford.edu

Yih-Tai Chen's current address is Cellomics, Inc., 635 William Pitt Way, Pittsburgh, PA 15238.

1. *Abbreviations used in this paper:* aa, amino acids; arm, armadillo; CYT, cytoplasmic; endo H, endoglycosidase H; GFP, green fluorescent protein; GPI, glycosylphosphatidylinositol; LDL, low density lipoprotein; TER, transepithelial electrical resistance; TM, transmembrane.

Boulan and Powell, 1992; Matter and Mellman, 1994; Weimbs et al., 1997). These motifs are located in the cytoplasmic domain and include tyrosine-based sorting signals of VSV-G (Thomas et al., 1993) and LDL receptor (LDL-R; Matter et al., 1992), non-tyrosine-based signals of the polymeric immunoglobulin receptor (pIgR; Casanova et al., 1991), and the di-leucine motif of Fc receptor (Hunziker and Fumey, 1994; Matter et al., 1994). It is noteworthy that these proteins are not known to associate with heterologous membrane protein binding partners or accessory proteins in the secretory pathway.

E-cadherin, a type-I single-span transmembrane protein, is an endogenous adhesion molecule of epithelial cells (Kemler, 1992). E-cadherin mediates cell-cell adhesion by calcium-dependent homotypic interactions between E-cadherin extracellular domains on opposing membranes of contacting cells (Nagafuchi et al., 1987). However, strong adhesion requires linkage of the cytoplasmic domain of E-cadherin to the actin cytoskeleton (Nagafuchi and Takeichi, 1988). This linkage is mediated by direct binding of  $\beta$ -catenin to the cytoplasmic domain of E-cadherin (Aberle et al., 1994; Jou et al., 1995); the minimal  $\beta$ -catenin binding site on E-cadherin is thought to be a 30-amino acid basic sequence in the middle of the cytoplasmic domain (Stappert and Kemler, 1994). In turn,  $\beta$ -catenin binds  $\alpha$ -catenin (Aberle et al., 1994; Jou et al., 1995), which links the cadherin/catenin complex directly (Rimm et al., 1995) or indirectly (Knudsen et al., 1995) to the actin cytoskeleton. The stoichiometry of the E-cadherin/ $\beta$ -catenin/ $\alpha$ -catenin complex is 1:1:1 (Ozawa and Kemler, 1992; Hinck et al., 1994a). Finally, evidence has accumulated that E-cadherin forms dimers through interactions between the extracellular and/or membrane proximal domains of adjacent proteins (Shapiro et al., 1995; Briher et al., 1996; Nagar et al., 1996; Yap et al., 1998). In polarized MDCK cells, E-cadherin is localized to the lateral membrane (Le Bivic et al., 1990; Shore and Nelson, 1991), and newly synthesized E-cadherin is preferentially sorted in the Golgi and delivered directly to the basal-lateral membrane (Le Bivic et al., 1990). Mechanisms regulating assembly of the cadherin/catenin complex and targeting of E-cadherin to its site of function at the lateral membrane domain are unknown.

We are interested in the relationship between intracellular trafficking of membrane proteins and cell-cell adhesion. Previous studies reported that  $\beta$ -catenin binds to the cytoplasmic domain of E-cadherin shortly after E-cadherin synthesis, while  $\alpha$ -catenin joins the complex later, probably after E-cadherin has reached the cell surface (Ozawa et al., 1990; Hinck et al., 1994a). Thus, unlike other type-I membrane proteins studied (see above), E-cadherin is sorted and targeted to the basal-lateral membrane in a stoichiometric complex with a cytosolic protein,  $\beta$ -catenin. This prompted us to explore the relationship between E-cadherin sorting to the basal-lateral membrane domain and assembly of the E-cadherin/ $\beta$ -catenin complex. There are two regions of the cytoplasmic domain of E-cadherin which are similar in amino acid sequence to previously identified basal-lateral sorting signals of LDL-R (Matter et al., 1992), i.e., a sequence motif of Y---XXX, where X is an acidic amino acid residue. The first putative sorting signal in E-cadherin is immediately proximal to the trans-

membrane domain and the other is at the extreme COOH terminus, also similar to the locations of the two sorting signals in LDL-R cytoplasmic domain (see Fig. 1). We show that despite these similarities, mutations of tyrosine to alanine in those two potential basal-lateral sorting signals in E-cadherin do not affect sorting of newly synthesized mutant E-cadherin in MDCK cells. Further dissection of the cytoplasmic domain of E-cadherin using a chimeric protein approach revealed that E-cadherin exit from the ER and efficient sorting to the basal-lateral membrane are coupled to assembly of the E-cadherin/ $\beta$ -catenin complex shortly after E-cadherin synthesis.

## Materials and Methods

### Antibodies

Monoclonal antibody against rat GP2 has been described previously (Mays et al., 1995) and was a gift from Dr. Anson Lowe (Stanford University). Monoclonal antibody KT3 against SV-40 large T antigen (MacArthur and Walter, 1984) was a gift from Dr. Gernot Walter (University of California, San Diego, CA). Polyclonal antibody against the cytoplasmic domain of cadherin has been described previously (Marrs et al., 1993). Monoclonal antibody against human CD7 (T3.3A1) was obtained from American Type Culture Collection.

### Recombinant cDNA Construction

Due to the numerous recombinant cDNA constructs used in this study and that some constructs are derivatives in nature, construction details are not described for all constructs but are available upon request (E-mail: etchen@cmgm.stanford.edu). Individual constructs were confirmed by restriction mapping and DNA sequencing (PAN facility, Stanford University).

**Plasmid for Expression of E-cad<sup>sol</sup>.** U-GFP, a previously unpublished plasmid based on CDM8 (Aruffo and Seed, 1987a,b), containing a fusion protein with the extracellular domain of canine E-cadherin jointed with green fluorescent protein (GFP), was the starting material. The chimeric coding region is flanked by Hind3 and Not1 sites at the 5' and 3' end, respectively, with a Xho1 site as a linker (reading frame CTC-GAG, Leu-Glu) between the E-cadherin extracellular domain and GFP. The majority of the cadherin region (Hind3-Xho1, 2.1 kb) is derived from a cDNA clone (Hind3-Bgl2, 1.9 kb). The small remaining portion of the cadherin extracellular domain (Bgl2-Xho1, 0.2 kb) was from a PCR product. The GFP region was replaced with a pair of complimentary oligonucleotides encoding for the epitope tag of KT3 (amino acid sequence KPPTP-PPEPET) and a stop codon, while retaining the Xho1 linker and the 3'-end Not1 site. The resulting plasmid is named U-SVLT1. The encoded soluble, KT3-tagged extracellular domain of canine E-cadherin is named E-cad<sup>sol</sup>. A PCR reaction was carried out to amplify the coding region of E-cadherin from the internal endogenous Bgl2 site to the end of the coding region (the stop codon was replaced with a Xho1 site), using canine E-cadherin cDNA (a gift from Dr. Lee Rubin, University College London, UK) as the template. Note that the PCR product contains a small part of the extracellular domain and the complete transmembrane and cytoplasmic domains of E-cadherin and, after restricting with Bgl2 and Xho1, was used to replace the Bgl2 and Xho1 portion of U-SVLT1, resulting in the plasmid U-SVLT2. Thus, U-SVLT2 encodes a complete canine E-cadherin fused with KT3 epitope tag through a Xho1 (Leu-Glu) linker. Further mutagenesis of the putative basal-lateral sorting signals was carried out by PCR reactions to amplify the region of the Bgl2/Xho1 of U-SVLT2, as detailed below.

**Plasmids for Expression of E-cad BL1, BL2, and BL12.** Plasmid U-SVLT3, which encodes the mutant protein E-cadherin BL2 (Y→A mutations in BL2), was generated by PCR using the pair of oligonucleotides Cad BL-P6 (5'-CGC GGG CCA GAT CTT CCC CCC AAC ACA TCT-3'; Bgl2 site is underlined) and Cad BL-P3 (5'-CGC GGG CTC GAG GTC GTC CTC GCC ACC GCC GGC CAT GTC CGC GAG CTT-3'; Nae1 site is underlined). Note that the mutations introduced were accompanied by the introduction of a Nae1 site. The PCR product was used to replace the Bgl2 and Xho1 portion of U-SVLT2. Plasmid U-SVLT5, which encodes the mutant protein E-cadherin BL1 (Y→A mutations in BL1), was generated

by PCR from three reactions. A complimentary pair of oligonucleotides, Cad BL-P4 (5'-GAC ACC CGG GAC AAT GTT GCA GCT GCA GAT GAA GAA GGA GGT GG-3') and Cad BL-P5 (5'-CCA CCT CCT TCT TCA TCT GCA GCT GCA ACA TTG TCC CGG GTG TC-3'), encode the (Y→A) mutations (italics in the sequences given above) and were synthesized. Note that the introduction of a Pst1 site (underlined, CTGCAG) accompanied the introduction of the mutations. Two PCR reactions were carried out with pairs of oligonucleotides Cad BL-P6 (sense) and Cad BL-P5 (anti-sense), Cad BL-P4 (sense) and Cad BL-P2 (antisense, 5'-GCG CCC CTC GAG GTC GTC CTC GCC ACC TCC-3'; Xho1 site is underlined). The reaction products were mixed and served as the template for the third reaction with a pair of oligonucleotides, Cad BL-P6 (sense), and Cad BL-P2 (antisense). The PCR product was subcloned and replaced the Bgl2-Xho1 portion of the U-SVLT2 to give rise to U-SVLT5.

The plasmid U-SVLT4 which encodes E-cadherin BL12 (Y→A mutation in BL1 and BL2) was constructed in an identical manner as that used to construct U-SVLT5, except oligonucleotide Cad BL-PL3 was used in place of Cad BL-P2. Note that in the series of plasmids U-SVLT3, 4, and 5, the identity of the introduced mutations were checked by the presence of the Pst1 and/or NaeI restriction sites.

**GP2S.** Amino acids (aa) 1–504 of the coding region of rat GP2 cDNA (a gift from Dr. Anson Lowe, Stanford University) was amplified by PCR with a stop codon introduced downstream to amino acid 504, and with Hind3 and Not1 sites added to the 5' and 3' ends, respectively. The PCR product was subcloned into CDM8 through Hind3 and Not1 sites and resulted in the plasmid, GP2S.

**GP2CAD1.** GP2CAD1 is a chimeric protein of rat GP2 in which the GPI modification signal has been deleted (named GP2ΔGPI), and the transmembrane domain and cytoplasmic domain of canine E-cadherin added. To create GP2CAD1, the following oligonucleotides were used as PCR primers: a pair of complimentary oligonucleotides with the COOH terminus sequence of rat GP2 (without the GPI modification signal) joined in-frame with canine E-cadherin transmembrane sequence (italic), GP2CAD1-1S (5'-CAG AAT CCT GAT ACC TCC *GCG CCT TAC GCC GAA GCA*-3') and GP2CAD1-3A (5'-*TGC TTC GGC GTA AGG CGC GGA GGT ATC AGG ATT CTG*-3'); an oligonucleotide hybridizing with the COOH terminus of canine E-cadherin, including the stop codon, GP2CAD1-2A (5'-CGC GGG GCG GCC GCT TTA GTC GTC CTC GCC ACC TCC); an oligonucleotide hybridizing with the NH<sub>2</sub> terminus of GP2, including the start codon, GP2-1S (5'-CGC GGG AAG CTT AGG ATG GTG GCT TGT GAC-3'). Primers GP2-1S and GP2CAD1-3A were used to amplify GP2 using a cDNA clone of rat GP2. Primer GP2CAD1-2A was used with primer GP2CAD1-1S to amplify the transmembrane and cytoplasmic domains of canine E-cadherin using a cDNA clone of canine E-cadherin as the template. The PCR products from the two reactions were mixed and used as template for amplification using oligonucleotides GP2-1S and GP2CAD1-2A as primers. The final PCR product was then subcloned into the Hind3-Not1 sites of CDM8, and the plasmid was named GP2CAD1. GP2CAD1 was then used as the template to create chimeric proteins in the following section.

**GP2CAD1 Truncation Mutants.** GP2CAD2, 4, 6, 7, 8, and 10 are simple truncation mutants of GP2CAD1. GP2CAD1 was used as the PCR template. Individual antisense oligonucleotides hybridizing with the 6 aa upstream to the desired truncation, with a stop codon and Not1 site, were used with the oligonucleotide primer GP2-3S (5'-CGC GGG CAA GTC GAC TTC GCA GTA GTG AAC C-3'), which hybridizes to the region of the endogenous Sal1 site (underlined in the sequence) close to the COOH terminus of GP2 coding region, for individual PCR reactions to amplify parts of the cytoplasmic domain of E-cadherin. The resulting PCR products were cloned into GP2CAD1 through Sal1-Not1 sites. The cytoplasmic domain carried by each chimeric protein is shown in the diagram in Fig. 4, and described in detail in the Results section.

GP2CAD3 is a loop-out mutant constructed using a method similar to that used in the construction of GP2CAD1. A pair of complimentary oligonucleotides with the sequence corresponding to aa 77–82 and 130–135 of the cytoplasmic domain of E-cadherin were joined. The primer pair was used with oligonucleotides GP2-3S and GP2CAD1-2A to create GP2CAD3 using recombinant PCR reactions identical to those used to construct U-SVLT4 and GP2CAD1.

The other loop-out mutants, GP2CAD5 and GP2CAD9, were constructed in a similar manner as follows: aa 83–129 (BB1) of the cytoplasmic domain of canine E-cadherin were PCR amplified using the canine cDNA clone as template with a Xho1 site added to the 5' end and a Not1 site added to the 5' end downstream to a stop codon. The PCR product was subcloned into CDM8FluTag (Chen et al., 1993) through Xho1 and Not1 sites and resulted in an in-frame fusion with the influenza virus

hemagglutinin tag. The resulting plasmid was named HA-BB1. A PCR reaction were carried out to amplify the GP2 and the transmembrane domain of E-cadherin from GP2CAD1 to replace the HA portion in HA-BB1. The resulting plasmid encodes the chimeric protein GP2CAD5, which comprises GP2 and the transmembrane domain of E-cadherin fused with 83–129 of the cytoplasmic domain through a Xho1 linker (Leu-Glu). GP2CAD9 was constructed similarly.

**CD7BB1.** A human CD7 cDNA clone, CD7-31 (a gift from Dr. Brian Seed, Harvard University Medical School), was in a CDM8-based expression vector (Aruffo and Seed, 1987b) and was used directly for transfection. CD7-31 was used as the template for PCR to amplify the complete coding region of CD7 with Hind3 and Xho1 sites added to the 5' and 3' ends, respectively. The amplified CD7 was subcloned into HA-BB1 through Hind3 and Xho1 site which generated an in-frame fusion of CD7 and BB1. The resulting plasmid was named CD7BB1.

**E-cad8.** E-cad8 is a canine E-cadherin deletion mutant with 116–151 (the most COOH-terminal 36 aa) of the cytoplasmic domain deleted. The deletion in cytoplasmic domain is equivalent to that in GP2CAD8. Oligonucleotides Cad BL-P6 (see above) and E-CAD8-A (5'-CGC GGG CTC GAG GCT CAG ACT AGC AGC TTC AGA-3', the Xho1 site is underlined) were used to perform PCR using canine E-cadherin cDNA as the template. The PCR product was restrited with Xho1 and Bgl2, and then was subcloned into the plasmid U-SVLT1 after the Bgl2 and Xho1 digestion. The ligation resulted in an in-frame fusion with KT3 epitope tag through the Xho1 site with Leu-Glu as a linker at the COOH terminus of the truncated E-cadherin.

## Cells and Transfection

MDCK clone IIG cells (Mays et al., 1995), maintained in DME supplemented with 10% fetal bovine serum, were transfected using the calcium phosphate method (Graeve et al., 1990) with pSV2neo (Southern and Berg, 1982) as the selection marker. G418 resistant (500 μg/ml) colonies were isolated using cloning rings, and individual clones were expanded and screened by immunofluorescence staining or Western blotting using appropriate antibodies. For each construct, multiple clones were isolated and characterized. No difference in immunofluorescence staining or Western blot profile was found among clones transfected with the same construct. All of the transfected MDCK cells used in this study developed transepithelial electric resistance (TER) similar to that of parental MDCK cells. Two independent clones of each construct were used for experiments.

## Metabolic Labeling, Immunoprecipitation, and Related Methods

To monitor intracellular trafficking of newly synthesized protein, cells were grown on 24-mm Transwell™ filters for 7 d, incubated in DMEM without Met and Cys for 1 h, and then labeled with 250 μCi <sup>35</sup>S-Met/Cys (Pro-Mix; Amersham) for the time specified in individual experiments (20 min or 1 h). To metabolically label proteins to steady state, cells were labeled with 250 μCi <sup>35</sup>S-Met/Cys supplemented with 1.5 μg/ml of methionine and 3.0 μg/ml of cysteine-HCl for 24 h before extraction. When required, membrane domain-specific biotinylation was performed using NHS-SS-Biotin (Pierce) as described previously (Hammerton et al., 1991). Labeled cells were extracted with Triton X-100 Lysis buffer (10 mM Tris-HCl, pH 7.5, 120 mM NaCl, 25 mM KCl, 2 mM EDTA, 2 mM EGTA, and 0.5% Triton X-100) or with 1× NDET extraction buffer (1% NP-40, 2% sodium deoxycholate, 66 mM Na-EDTA, and 10 mM Tris-HCl, pH 7.4). After treating with specific antibody bound on protein A-Sepharose (Pharmacia), immunoprecipitates were washed with High Stringency Buffer (HS-B): 20 mM Tris-HCl, pH 7.5, and 120 mM NaCl, 25 mM KCl; 5 mM EDTA; 5 mM EGTA; 0.1% SDS; 1% Na-deoxycholate; 0.5% Triton X-100, and High Salt Wash Buffer (HS-B containing 1 M NaCl). If cells were biotinylated before extraction, biotinylated immunoprecipitates were collected with immobilized avidin (Pierce) as described previously (Hammerton et al., 1991). Samples were then resolved by SDS-PAGE and radioactive signals were collected by fluorography or a PhosphorImager (Molecular Dynamics). Signals were quantified with a PhosphorImager or a laser densitometer (Hoefer, San Francisco, CA).

To perform digestion of GP2CAD10 with endoglycosidase H, GP2CAD10 MDCK cells were grown on 24-mm Transwell™ filters for 7 d, labeled with 250 μCi of <sup>35</sup>S-Met/Cys for 24 h, then extracted with 1× NDET and immunoprecipitated with the monoclonal antibody against rat GP2. Immunoprecipitates were released from protein A-Sepharose (Pharmacia) and antibodies by boiling in 50 μl of 1% SDS, 200 mM

dithiothreitol for 5 min. An equal volume of 100 mM citric acid buffer (pH 5.5) was added to the immunoprecipitates, and 1 U of endoglycosidase H (Boehringer Mannheim) was added and the sample was incubated at 37°C for 16 h. The processed samples were resolved by 10% SDS-PAGE and detected by fluorography.

Radioactive signals collected with a PhosphorImager were transferred directly to Adobe Photoshop, and radioactive signals collected with fluorography were scanned from autoradiography film (Kodak) into Adobe Photoshop with a Hewlett-Packard Scan-Jet IIc scanner. The contrast of images was adjusted in Photoshop, the images were arranged and labeled for individual figures using Canvas 5 (Deneba Software). In some cases, samples containing apical or basal-lateral membrane biotinylated proteins were separated in gels with an empty lane between the sample lanes in order to avoid any cross contamination of protein samples. The empty, intervening lane was removed in Canvas 5 and the two sample lanes are shown side-by-side. The rearranged images were printed using a Tektronix dye sublimation printer. The printed images are representative of the original data.

### Size Exclusion Chromatography

Preparation of samples and elution of extracted proteins of MDCK cells from Superose 6 column was performed using identical procedures as previously published (Stewart and Nelson, 1997). The collected fractions were resolved by 7.5% SDS-PAGE and proteins were transferred onto nitrocellulose membranes. The membranes were then probed with a monoclonal antibody against the extracellular domain of E-cadherin (Transduction Laboratories) or a monoclonal antibody against  $\beta$ -catenin (Transduction Laboratories). After incubation with horseradish peroxidase conjugated secondary antibody (Amersham), the signals were recorded using ECL reagent (Amersham) and autoradiography film (Kodak).

### Immunofluorescence Staining and Other Staining Methods

For immunofluorescent staining of GP2 chimeric proteins, cells on collagen coated coverslips were fixed with 3.7% paraformaldehyde in 0.1 M phosphate buffer (pH 7.2) at room temperature, permeabilized with 0.5% Triton X-100 in PBS, and processed for immunofluorescence staining with monoclonal antibody against rat GP2. NBD-ceramide (Molecular Probes) staining of the Golgi apparatus performed on fixed MDCK cells as published previously (Pagano et al., 1989). Acridine orange staining of lysosomes in live MDCK cells on coverslips was performed by adding acridine orange (1  $\mu$ g/ml; Sigma Chemical Co.) to growth medium for 30 min at 37°C, followed by incubation in normal growth medium without acridine orange for 15 min. Then the coverslip was then mounted on a microscope slide with spacers to form a chamber for direct observation.

Fluorescent antibody-stained cells, NBD-ceramide-stained fixed cells, or acridine orange stained living cells were observed using a Zeiss AxioPlan fluorescence microscope with a 63 $\times$  objective and the appropriate filter sets. Note that for observation of acridine orange staining, the normal filter set for fluorescein isothiocyanate fluorescence was reconfigured by replacing the barrier filter with a long pass band filter (590 nm). Fluorescent images of stained cells were recorded using Kodak Tri-X film (see Fig. 5 A) or Kodak Ektachrome Elite II (ASA 400) film (see Fig. 5, B–D). Photographic images were then digitized with a slide scanner (Nikon) and resized using Adobe Photoshop. Images in Fig. 5 and Fig. 12 were arranged and labeled using Canvas 5 and printed from the computer file using a dye sublimation printer.

## Results

### LDL-R-like Basal-lateral Sorting Motifs Are Not Responsible for Basal-lateral Sorting of E-Cadherin

The primary structure of the cytoplasmic domain of E-cadherin contains two regions with amino acid sequences and spacing that are similar to previously identified basal-lateral sorting signals in the cytoplasmic domain of the LDL-R (Matter et al., 1992; see Fig. 1). We assessed whether these two motifs function as basal-lateral sorting determinants for E-cadherin. All tyrosine residues in each

### LDL-R

```

1      18      37
[TM] KNWR.....YQKTTTEDE.....YSPSRQMVSLIEDDVA end
          |           |           |
          Y           EDE          Y           EDD

```

### E-cadherin

```

1      22      145
[TM] RRRVV.....YYDEEGGGEED.....YGGGEED end
          |           |           |
          Y           EED          Y           EDD
          [ BL1 ]           [ BL2 ]

```

[TM] = transmembrane domain  
 [BL1] = putative basal-lateral sorting determinant 1  
 [BL2] = putative basal-lateral sorting determinant 2

**Figure 1.** Amino acid sequence comparison of the basal-lateral membrane sorting determinants in human LDL receptor (Matter et al., 1992), and putative basal-lateral sorting determinant(s) in the cytoplasmic domain of canine E-cadherin.

motif of canine E-cadherin were mutated into alanine in region 1 (BL1), or region 2 (BL2), or both (BL12); similar mutations in both motifs of LDL-R resulted in random sorting to the cell surface in MDCK cells (Matter et al., 1992). Each mutant was epitope-tagged with the SV-40 large T antigen epitope (KT3 tag, amino acid sequence KPPTPPPEPET; see MacArthur and Walter, 1984) and stably transfected into MDCK cells (Fig. 2). Confluent monolayers of cells were grown on Transwell™ filters for 7 d, and then labeled with <sup>35</sup>S-Met/Cys for 1 h. At the end of the 1 h labeling period, the first wave of newly synthesized E-cadherin that arrived at the apical or basal-lateral membrane (Shore and Nelson, 1991) was detected by cell surface biotinylation. Mutant E-cadherin was distinguished from endogenous E-cadherin with the KT3 monoclonal antibody to the epitope tag.

Greater than 95% of newly synthesized mutant E-cadherin, lacking tyrosine residues in either region 1 (BL1), or region 2 (BL2), or both (BL12) was delivered to the basal-lateral domain of MDCK cells with an efficiency and fidelity similar to those of endogenous E-cadherin (Fig. 2). This result indicates that the basal-lateral sorting determinant(s) of E-cadherin are different from those of LDL-R. To further dissect basal-lateral sorting determinants in E-cadherin, we next examined the overall localization of the basal-lateral sorting determinant in the whole molecule.

A secreted form of E-cadherin (E-cad<sup>sol</sup>), in which the transmembrane (TM) and cytoplasmic (CYT) domains had been deleted, was expressed stably in MDCK cells (Fig. 2). Delivery of newly synthesized E-cad<sup>sol</sup> to different membrane domains was detected by sampling apical and basal-lateral medium for <sup>35</sup>S-Met/Cys labeled E-cad<sup>sol</sup>. Note that E-cad<sup>sol</sup> was efficiently secreted into the culture medium, did not associate with the cell surface of MDCK cells, and did not disrupt TER (Y.-T. Chen, unpublished result). As shown in Fig. 2, newly synthesized E-cad<sup>sol</sup> was secreted equally into the medium of both apical and basal-lateral compartments of the Transwell™ filter. We conclude that the extracellular domain of E-cadherin does not carry signals that specify E-cadherin sorting or delivery to the basal-lateral membrane.

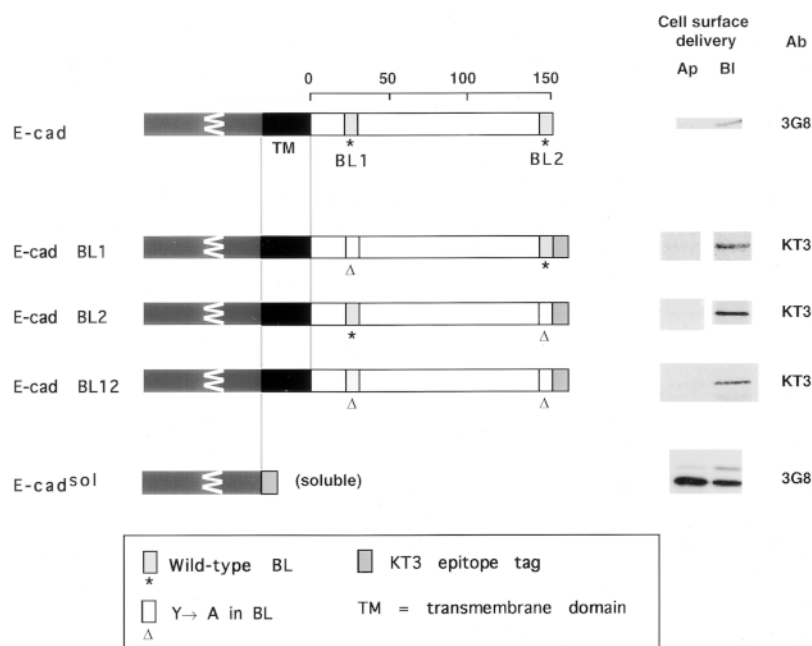


**Figure 2.** Delivery of newly synthesized KT3 tagged E-cadherin mutants to the basal-lateral membrane domain, and secretion of E-cad<sup>sol</sup> into both apical and basal-lateral media. The diagram shows schematically the structure of each mutant constructs. The scale shows the number of amino acid residues in the cytoplasmic domain (CYT); the extracellular domain is not drawn to the same scale. To examine plasma membrane delivery, cells expressing E-cadherin (E-cad), or tyrosine to alanine substitution mutants (E-cad BL1, BL2, and BL12) were grown on Transwell<sup>TM</sup> filters for 7 d, labeled with <sup>35</sup>S-Met/Cys for 1 h, cell surface biotinylated on either the apical (Ap) or basal-lateral (BI) membrane, and then processed for immunoprecipitation using the specified antibodies (mAb KT3 against epitope tag, or 3G8 against the extracellular domain of canine E-cadherin) followed by immobilized avidin. Secretion of E-cad<sup>sol</sup> was assessed in confluent cell monolayers grown on Transwell<sup>TM</sup> filters by sampling the apical and basal-lateral media for <sup>35</sup>S-Met/Cys protein.

### Basal-lateral Sorting Activity Resides in the Cytoplasmic Domain of E-Cadherin

To locate the basal-lateral sorting signal(s) in E-cadherin, we constructed a chimeric protein comprising the transmembrane and specific regions of the cytoplasmic domain of E-cadherin fused to the extracellular domain of GP2, a highly glycosylated protein of zymogen granules in pancreatic exocrine cells (Hoops and Rindler, 1991). Normally, GP2 is attached to the membrane via a GPI anchor, and is delivered exclusively to the apical domain of MDCK clone II/G cells (Mays et al., 1995). A deletion mutant of GP2 that lacked the GPI modification signal (Fig. 3 A, GP2ΔGPI) was expressed in MDCK cells. As shown in

Fig. 3 A, newly synthesized GP2ΔGPI was secreted equally into both the apical and basal-lateral medium. This result confirms that GP2 sorting to the apical membrane requires the GPI-anchor (see Mays et al., 1995), and reveals that the extracellular domain of GP2 does not contain specific sorting signals for the basal-lateral membrane.

GP2ΔGPI was fused to the TM and CYT of E-cadherin, producing the chimeric protein GP2CAD1 (Fig. 3 B). Significantly, >95% of newly synthesized GP2CAD1 was preferentially delivered to the basal-lateral domain, which represents an efficiency and fidelity of delivery similar to that of endogenous E-cadherin. We conclude the transmembrane and cytoplasmic domains of E-cadherin contain a basal-lateral sorting signal(s).

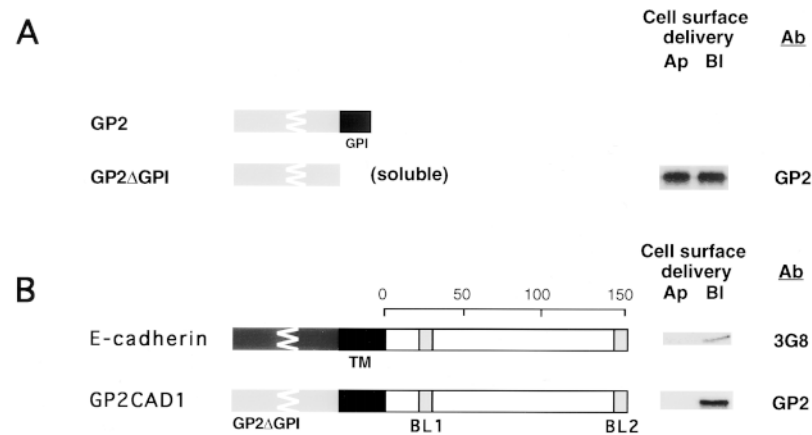


**Figure 3.** Dominant basal-lateral sorting activity of E-cadherin is located in the transmembrane/cytoplasmic domains. (A) GPI modification is the sole determinant for targeting GP2 to the apical membrane. GP2 has been shown previously to be preferentially delivered to the apical domain of MDCK clone II/G cells (Mays et al., 1995). Diagrams show schematically the structure of GP2 lacking the GPI modification signal (GP2ΔGPI). GP2ΔGPI delivery was determined as described for E-cad<sup>sol</sup> (see Fig. 1 legend, and Materials and Methods). (B) Newly synthesized GP2CAD1, labeled for 1 h, is sorted to the basal-lateral membrane domain, similar to endogenous E-cadherin. Diagrams show schematically the structure of GP2CAD1 compared with E-cadherin. GP2CAD1 delivery to the cell

surface was assessed by <sup>35</sup>S-Met/Cys labeling and cell surface biotinylation of the apical (Ap) or the basal-lateral (BI) membrane domain. Note that the autoradiogram showing the E-cadherin targeting is the same as that shown in Fig. 2, and is included here for comparison.

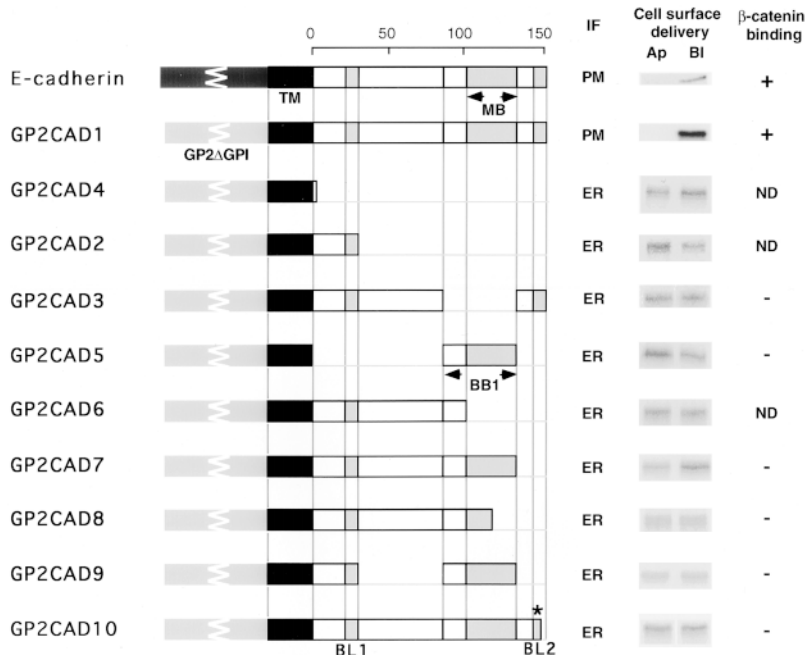


**Figure 4.** Truncations of the cytoplasmic domain of E-cadherin result in accumulation of mutant proteins in the ER. Diagrams show schematically the structure of GP2/E-cadherin cytoplasmic domain chimeric constructs (GP2CAD1–10). E-cadherin and GP2CAD1 diagrams are included for comparison. E-cadherin and GP2CAD1 data from Figs. 2 and 3 are included for comparison. Immunofluorescence (IF) revealed plasma membrane (PM) staining for E-cadherin and GP2CAD1 while all other chimeric proteins (GP2CAD2–10) gave an intracellular reticular staining pattern consistent with localization in the endoplasmic reticulum (ER). Examples of staining are given in Fig. 5. 1 h labeling with <sup>35</sup>S-Met/Cys and cell surface biotinylation show delivery of newly synthesized chimeric protein to both apical (Ap) and basal-lateral (Bl) membrane domains. β-catenin binding to GP2CAD1 and derived mutant proteins was assessed by steady state <sup>35</sup>S-Met/Cys labeling for 24 h and immunoprecipitation using anti-GP2 antibody. Examples of immunoprecipitates of GP2CAD1, 3, 7, 8, and 10 are given in Fig. 9. Catenin binding was not determined (ND) for GP2CAD2, 4, and 6, because these proteins completely lacked the minimal β-catenin binding domain (see text).

### Systematic Deletions of E-Cadherin Cytoplasmic Domain Result in Retarded Exit from ER and Random Delivery of GP2/Cadherin Chimera to the Apical and Basal-lateral Cell Surface

To map in detail the basal-lateral sorting domain of E-cadherin, a series of chimeric proteins were created in which GP2ΔGPI was used as the extracellular domain (reporter) fused to the transmembrane domain and specific regions of the cytoplasmic domain of E-cadherin (Fig. 4). Each mutant was designed to explore whether distinct features/activities of the cytoplasmic domain, such as binding to β-catenin and individual putative sorting signals, could be separated from each other.

In general, two types of deletion mutants were constructed. The first type involved the introduction of simple truncations in the cytoplasmic domain: GP2CAD2 contained amino acids (aa) 1–33 of the cytoplasmic domain, and ended at the COOH terminus of the first putative basal-lateral sorting signal (BL1); GP2CAD4 only contained the first 4 aa of the cytoplasmic domain; GP2CAD6 contained aa 1–99 of the cytoplasmic domain, and ended just before the start of the previously defined minimal β-catenin binding domain (see Introduction); GP2CAD7 contained aa 1–129 of the cytoplasmic domain, and ended at the COOH terminus of the minimal β-catenin binding domain (aa 100–129); GP2CAD8 contained aa 1–115 of the cytoplasmic domain, and ended in the middle of the minimal β-catenin binding domain; GP2CAD10 contained almost all of the cytoplasmic domain except the COOH-terminal three acidic amino acids (EDD). The second type of mutants were loop-out mutants in which two halves of the cytoplasmic domain were joined after an intervening

sequence had been deleted: GP2CAD3 contained a deletion of aa 83–129 of the cytoplasmic domain (minimal β-catenin binding domain is aa 100–129); GP2CAD5 contained aa 83–129 of the cytoplasmic domain; GP2CAD9 contained aa 1–33 and aa 83–129 of the cytoplasmic domain. Rather unexpectedly, none of the mutants (GP2CAD1–GP2CAD10) gave distinct sorting patterns compared with endogenous E-cadherin or GP2CAD1 (Fig. 4). In all cases, mutant proteins were delivered equally to both apical and basal-lateral membranes. Note that the relative amounts of each chimera delivered to either the apical or basal-lateral membrane domain are directly comparable, but a comparison cannot be made between the amount of cell surface delivery of different chimeras from these data. However, as described above, with the exception of E-cadherin and GP2CAD1, the amount of each chimera that reached the cell surface was <10% of that synthesized.

To examine the subcellular location of each chimeric protein, cells were grown on glass coverslips and processed for immunofluorescence. An anti-GP2 antibody was used to examine the distributions of the GP2CAD chimeras, and to distinguish them from endogenous E-cadherin. As shown in Fig. 5 A, GP2CAD1 was localized mainly at the cell surface, including cell–cell contact sites, similar to endogenous E-cadherin. In contrast, staining of all other chimeric proteins (GP2CAD2–GP2CAD10) revealed an intracellular, reticular staining pattern; only staining for GP2CAD10 is shown in Fig. 5 B, but the staining of other chimeric proteins (GP2CAD2–GP2CAD9) was indistinguishable from that of GP2CAD10 (Y.-T. Chen, unpublished results). In addition, larger, punctate structures

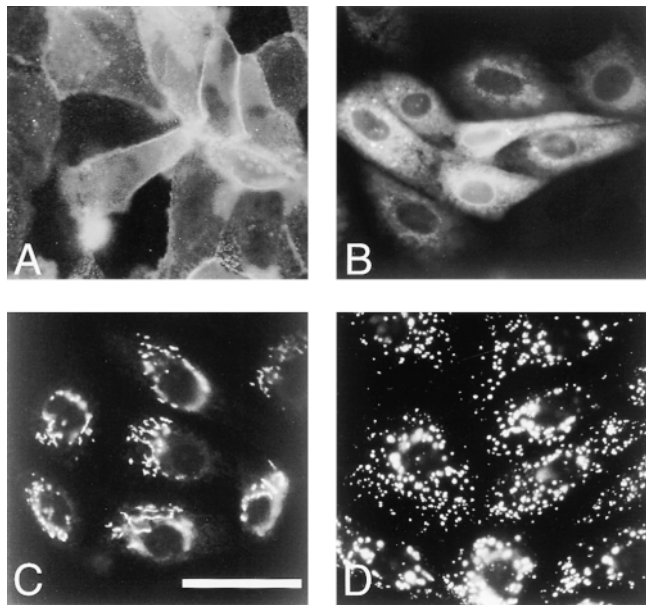


**Figure 5.** GP2CAD1 and GP2CAD10 show differences in subcellular localization by immunofluorescence staining. Reticular staining of GP2CAD10 (B) is distinct from cell surface staining of GP2CAD1 (A), Golgi staining (C), and lysosomal staining (D). Monoclonal antibody against rat GP2 was used to stain GP2CAD1 (A) and GP2CAD10 (B) expressing MDCK cells; (C) NBD-ceramide staining of paraformaldehyde-fixed MDCK cells; (D) Acridine orange staining of living MDCK cells. Bar, 50  $\mu$ m.

were stained for GP2CAD10. The reticular pattern of GP2CAD10 staining (Fig. 5 B), and other GP2CAD mutants was very similar to that of the ER resident protein BiP in MDCK cells (Bush et al., 1997). It was distinct from the Golgi revealed by NBD-ceramide staining of fixed cells (Fig. 5 C; Pagano et al., 1989), and lysosomes revealed by labeling live cells with acridine orange (Fig. 5 D; Palmgren, 1991). Thus, the majority of GP2CAD10 is most likely localized to the ER.

To confirm biochemically that GP2CAD1 deletion mutants were retained in the ER, we examined the sensitivity of GP2CAD10 to digestion by endoglycosidase H (endo H). GP2CAD10 MDCK cells were incubated with  $^{35}$ S-Met/Cys for 24 h to label proteins to steady state. Total cell lysates were prepared, and GP2CAD10 was immunoprecipitated with anti-GP2 antibody and then subjected to endo H digestion. As shown in Fig. 6, endo H digestion resulted in a significant increase in electrophoretic mobility of the major GP2CAD10 protein band. Note that the electrophoretic mobility of a minor protein band (Fig. 6, asterisk) was not affected by incubation with endo H. This upper band appears to be specific to the GP2 antibody as a minor protein with a slower electrophoretic mobility was also present in other GP2 chimeric protein immunoprecipitates. It is likely that this protein band represents a small portion ( $\sim$ 10%) of the chimeric protein that exited the ER and had undergone processing in the Golgi to remove the high mannose carbohydrate chain. From the data on the sensitivity of GP2CAD10 to endo H digestion, we conclude that at steady state  $>$ 85% of GP2CAD10 retained

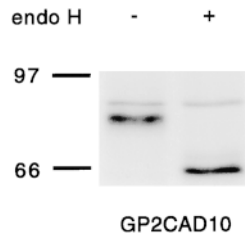


**Figure 6.** The majority of GP2CAD10 is sensitive to endoglycosidase H digestion. GP2CAD10 expressing MDCK cells were grown on Transwell™ filters for 7 d, labeled with  $^{35}$ S-Met/Cys for 24 h, extracted and immunoprecipitated with GP2 antibody. Immunoprecipitates were incubated in the presence (+) or absence (-) of endo H, and were subsequently resolved by SDS-PAGE and detected by fluorography. Only a small fraction ( $\sim$ 10%) of GP2CAD10 (marked with asterisk) does not display an increase in electrophoretic mobility upon endo H treatment. Numbers at the left show molecular mass in kD.

high mannose carbohydrate chains and had not undergone further processing consistent with its location in the ER.

### **Truncations of E-Cadherin Cytoplasmic Domain Result in both Reduced Cell Surface Delivery and Random Sorting to Plasma Membrane Domains**

The difference in staining patterns of GP2CAD1 and GP2CAD10 (Fig. 5) might reflect differences in the efficiency of protein passage through the secretory pathway. Therefore, we compared the kinetics of cell surface delivery of newly synthesized GP2CAD1, GP2CAD10, and endogenous E-cadherin (Fig. 7). MDCK cells stably expressing GP2CAD1 or GP2CAD10 were grown on Transwell™ filters for 7 d, pulse labeled with  $^{35}$ S-Met/Cys for 20 min, and chased in DMEM containing an excess of nonradioactive Met/Cys for 40 min. At the end of the chase period, either whole cell lysates were collected, or cells were treated with the plasma membrane-impermeant biotinylating agent NHS-SS-biotin before lysis. Cell lysates were immunoprecipitated with antibody specific to rat GP2; biotinylated proteins were further precipitated with immobilized avidin. Identical experiments were performed with parental MDCK cells to examine the kinetics of endogenous E-cadherin delivery to the plasma membrane.

As shown in Fig. 7 A,  $25.9 \pm 1.3\%$  of newly synthesized endogenous E-cadherin,  $23.0 \pm 1.8\%$  of GP2CAD1, and  $6.8 \pm 3.1\%$  of GP2CAD10 reached the cell surface. Note that the percentage of protein detected by cell surface biotinylation represented only the fraction of newly synthesized protein delivered from the ER to the plasma membrane in the 40-min chase period. Thus, the amount of GP2CAD1 delivered to the cell surface was similar to that of endogenous E-cadherin, while the amount of GP2CAD10 delivered to the cell surface was considerably lower than that of either GP2CAD1 or E-cadherin.

The difference in the amount of cell surface delivery of GP2CAD10 and GP2CAD1 (or endogenous E-cadherin) was also reflected in the steady state distribution of these proteins (Fig. 7 B). GP2CAD1 and GP2CAD10 expressing cells were labeled with  $^{35}$ S-Met/Cys to steady state for 24 h. Parallel cultures were either extracted immediately, or biotinylated on both apical and basal-lateral membranes. Biotinylated and non-biotinylated proteins were isolated as described above. As shown in Fig. 7 B, the amount of biotinylated cell surface GP2CAD1 was  $\sim$ 90%

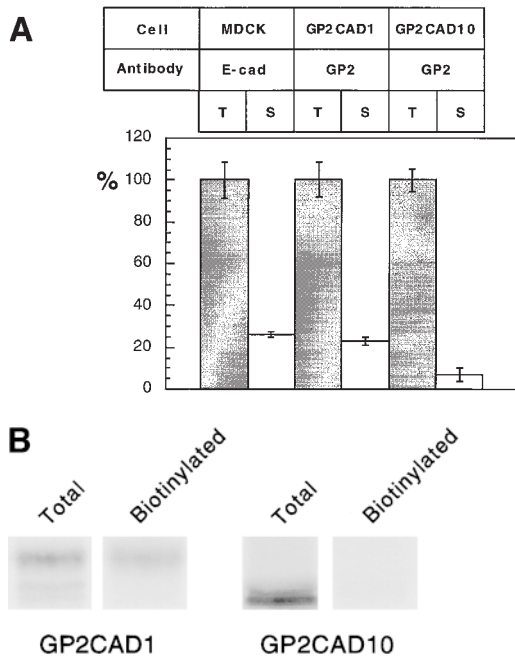


**Figure 7.** Rate of E-cadherin and GP2CAD1 delivery to the cell surface are similar, while GP2CAD10 is delivered to the cell surface at a reduced rate. At steady state, the majority of GP2CAD1 is on plasma membrane, while the majority of GP2CAD10 is intracellular. (A) Arrival of newly synthesized proteins on cell surface monitored by cell surface biotinylation. Cells were labeled with  $^{35}\text{S}$ -Met/Cys for 20 min, chased for 40 min, cell surface biotinylated, lysed, and immunoprecipitated with antibodies to either E-cadherin (E-cad) or GP2. Aliquots of cell surface protein (S, biotinylated, open columns) were normalized to the amount of protein in total cell lysate (T, shaded columns). Error bars show standard deviation ( $n = 3$ ). (B) Steady state distribution of GP2CAD1 and GP2CAD10. Cells were labeled with  $^{35}\text{S}$ -Met/Cys for 24 h, surface biotinylated on both apical and basal membranes, extracted and immunoprecipitated; biotinylated proteins were retrieved with immobilized avidin. Results show that 91.3% ( $\pm 1.3\%$ ,  $n = 2$ ) of GP2CAD1 is on the cell surface, but  $\sim 7.2\%$  ( $\pm 0.8\%$ ,  $n = 2$ ) of GP2CAD10 is on cell surface.

of the total GP2CAD1 extracted from cells. In contrast, the amount of biotinylated GP2CAD10 was  $\sim 7\%$  of the total amount of GP2CAD10. Since the extracellular domain of GP2CAD1 and GP2CAD10 were identical, the difference in the amount of cell surface exposed proteins is unlikely to be due to a difference in the efficiency of protein biotinylation. We conclude that GP2CAD1 rapidly and efficiently exits the ER and is delivered to the basal-lateral membrane. In contrast,  $\sim 90\%$  of GP2CAD10 is retained in the ER, while the remainder slowly leaks out into the secretory pathway and is delivered to both apical and basal-lateral membranes.

#### Effects of aLLN and Chloroquine on GP2CAD1 and GP2CAD10 Degradation

The data presented above show that nearly all of GP2CAD10 is retained in the ER, whereas nearly all GP2CAD1 is localized in the plasma membrane. It is generally acknowledged that misfolded secretory proteins retained in the ER are degraded through the proteasome

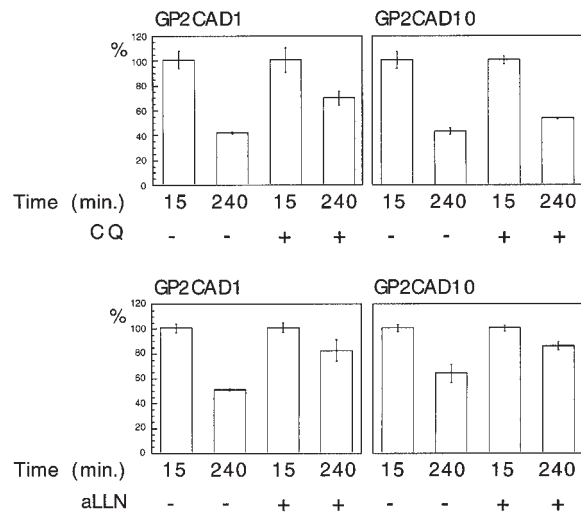


**Figure 8.** Effects of chloroquine phosphate (top panels) and aLLN (bottom panels) on the degradation of GP2CAD1 (left panels) and GP2CAD10 (right panels). Chloroquine phosphate (CQ, 0.1 mM) treatment of cells started 1 h before pulse labeling with  $^{35}\text{S}$ -Met/Cys (15 min), and aLLN (25  $\mu\text{M}$ ) treatment started 3 h before pulse labeling with  $^{35}\text{S}$ -Met/Cys (15 min). At the end of the pulse labeling (15 min) or chase period (240 min, 15-min pulse labeling, and 225-min chase), cells were extracted with  $1\times$  NDET, and protein was immunoprecipitated with an antibody against rat GP2. Data for each column were from two 24-mm Transwell<sup>TM</sup> filters and the error bars show the range of the data.

pathway (for a recent review, see Coux et al., 1996). To examine degradative pathways, cells were pulse-labeled with  $^{35}\text{S}$ -Met/Cys for 15 min and then chased in an excess of nonradioactive Met/Cys for 225 min in the presence of either chloroquine phosphate (a lysosome inhibitor) or N-acetyl-Leu-Leu-norleucinal (aLLN, a 26S proteasome inhibitor). As shown in Fig. 8 (upper panels), 70% of newly synthesized GP2CAD1 remained at the end of the chase period in the presence of chloroquine, compared with 40% in its absence. By comparison,  $\sim 50\%$  of GP2CAD10 remained in the presence of chloroquine compared with 42% in its absence. In the presence of aLLN (Fig. 8, bottom panels), 82% of GP2CAD1 remained compared with 50% in its absence; 83% of GP2CAD10 remained in the presence of aLLN, compared with 60% in its absence. These results show that chloroquine phosphate suppressed degradation of both GP2CAD1 and GP2CAD10 but the effect on GP2CAD1 was greater. On the other hand, aLLN had a more inhibitory effect on the degradation of GP2CAD10 than did chloroquine, while both aLLN and chloroquine suppressed the degradation of GP2CAD1.

#### E-Cadherin Binding to $\beta$ -Catenin Is Coupled to Efficient ER Exit and Basal-lateral Membrane Delivery

The GP2CAD1 mutants were designed to test whether binding of  $\beta$ -catenin to the cytoplasmic domain of E-cadherin and basal-lateral membrane delivery could be separated from each other. GP2CAD1, GP2CAD5, GP2CAD7, GP2CAD9, and GP2CAD10 (see Fig. 4) were predicted to bind  $\beta$ -catenin since they contained at least aa

83–129 of the cytoplasmic domain of E-cadherin which covers the previously defined minimal  $\beta$ -catenin binding domain (aa 100–129; Stappert and Kemler, 1994).

The GP2CAD1/catenin complex was coimmunoprecipitated with GP2 antibody and subjected to a high stringency wash in buffer containing 0.1% SDS, 1% sodium deoxycholate, and 1 M NaCl (High Stringency Wash Buffer, see Materials and Methods). Note that under this wash condition the stoichiometry of the coimmunoprecipitated complex of GP2CAD1/ $\beta$ -catenin/ $\alpha$ -catenin was  $\sim$ 1:1 (Fig. 9), similar to that of the endogenous E-cadherin/catenin complex (Ozawa and Kemler, 1992; Hinck et al., 1994a; see also Fig. 10). Surprisingly, we found that neither GP2CAD10 nor GP2CAD7 bound catenins under these conditions (Fig. 9), although both chimeras contained the previously mapped minimal  $\beta$ -catenin binding domain of E-cadherin (see Fig. 4). Similar results were obtained with GP2CAD5 and GP2CAD9 (Y.-T. Chen, unpublished results). Catenins were not coimmunoprecipitated in a complex with either GP2CAD8 (Fig. 9) in which the COOH-terminal half of the  $\beta$ -catenin binding domain had been deleted, or GP2CAD3 (Fig. 9) in which the  $\beta$ -catenin binding domain had been completely deleted. Overall, there is a strong correlation between lack of  $\beta$ -catenin binding to the cytoplasmic domain of E-cadherin, and retention of the majority of each GP2CAD1 mutant in the ER. Note that Fig. 9 also reveals a difference in the apparent molecular mass of GP2CAD1 and all other GP2CAD mutants. It is likely that this is due to differences in complex carbohydrate modifications between the proteins. GP2 is known to undergo extensive N-linked glycosylation (Hoops and Rindler, 1991). We show here that GP2CAD1 is efficiently delivered to cell surface and, thereby, receives extensive carbohydrate modifications during trafficking through the secretory pathway. In contrast, all other GP2CAD mutants are retained in the ER and, therefore, do not undergo complex carbohydrate modifications.

We also examined  $\beta$ -catenin binding to E-cadherin mutants in which putative basal-lateral sorting motifs has been mutated (Tyr $\rightarrow$ Ala), and an E-cadherin chimera formed with another protein, human CD7. Stable MDCK

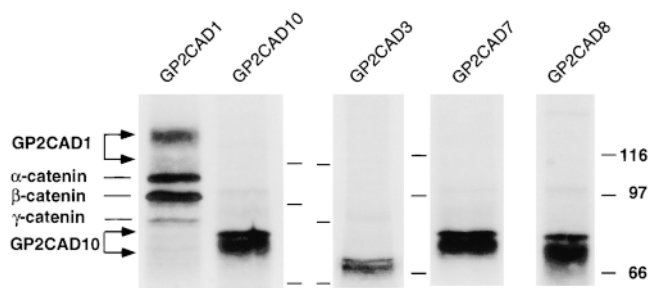


**Figure 9.** Catenins bind to GP2CAD1 but not GP2CAD3, GP2CAD7, GP2CAD8, or GP2CAD10. MDCK cells expressing individual constructs were grown on Transwell™ filters for 7 d, labeled with  $^{35}\text{S}$ -Met/Cys for 24 h, extracted, and proteins were immunoprecipitated with GP2 antibody. Immunoprecipitates were resolved by 10% SDS-PAGE. Markings to the right of columns for GP2CAD10 and GP2CAD8, and those to the left of columns of GP2CAD3 and GP2CAD7 show the positions of molecular mass markers; 116, 97, and 66 kDa.

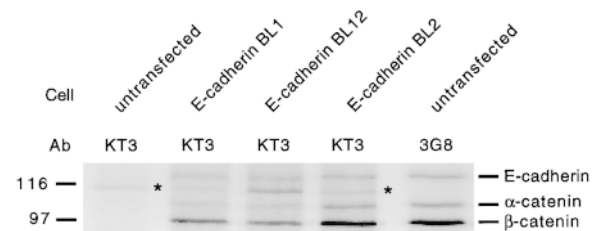
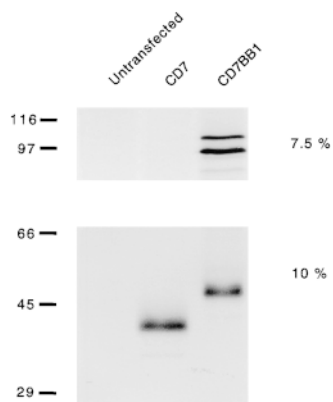


**Figure 10.** Catenins bind to E-cadherin and epitope tagged (Tyr $\rightarrow$ Ala) E-cadherin mutants. Parental MDCK cells or cells expressing individual mutant E-cadherins were grown on Transwell™ filters for 7 d, labeled for 24 h with  $^{35}\text{S}$ -Met/Cys, extracted, and immunoprecipitated with either mAb 3G8 (against the extracellular domain of canine E-cadherin) or mAb KT3 (against KT3 tag). Note that KT3 antibody immunoprecipitated nonspecifically a protein band with apparent molecular mass of  $\sim$ 112 kDa in untransfected cells (marked with asterisk). In cells expressing KT3 tagged E-cadherin mutants, specific bands corresponding to E-cadherin,  $\alpha$ -catenin, and  $\beta$ -catenin were detected.

cell lines expressing E-cadherin BL1, E-cadherin BL2, or E-cadherin BL12 were labeled with  $^{35}\text{S}$ -Met/Cys to steady state for 24 h, and mutant proteins were immunoprecipitated with the monoclonal antibody KT3 under the stringent wash conditions used above. All three Tyr-to-Ala mutants of E-cadherin (BL1, BL2, and BL12) bound  $\beta$ -catenin and  $\alpha$ -catenin under high stringency wash conditions (Fig. 10); note that these mutants were rapidly exported from the ER and sorted efficiently and specifically to the basal-lateral membrane (Fig. 2).

We placed the putative minimal  $\beta$ -catenin binding domain (aa 83–129, BB1) of E-cadherin cytoplasmic domain on the COOH terminus of an unrelated type-I transmembrane protein, human CD7. The resulting chimeric protein (CD7BB1) bound  $\alpha$ -catenin and  $\beta$ -catenin, whereas CD7 did not (Fig. 11; note that aliquots of the sample were resolved by either 7.5% or 10% SDS-PAGE in order to obtain better separation of  $\alpha$ -catenin/ $\beta$ -catenin and CD7/CD7BB1, respectively). However, quantification of the amounts of  $\alpha$ - and  $\beta$ -catenins bound to CD7BB1 revealed that the stoichiometry of CD7BB1/ $\beta$ -catenin/ $\alpha$ -catenin was 5:1:0.8 when normalized to the number of Met and Cys residues in CD7BB1 and catenins; this compared with the ratio of  $\sim$ 1:1:1 for E-cadherin/ $\beta$ -catenin/ $\alpha$ -catenin or GP2CAD1/ $\beta$ -catenin/ $\alpha$ -catenin (see above). Most of CD7 and CD7BB1 was localized at the cell surface (Y.-T. Chen, unpublished results); presumably, the cytoplasmic domain of CD7 in the CD7BB1 chimera contains signal(s) for its entry into the secretory pathway regardless of whether  $\beta$ -catenin is bound or not. Trafficking patterns of CD7 and CD7BB1 were similar in polarized MDCK cells. Approximately 60% of the cell surface delivery of both proteins was to the basal-lateral membrane (Y.-T. Chen, unpublished results). We conclude that a domain containing aa 83–129 is a transportable  $\beta$ -catenin binding domain in E-cadherin, but the binding strength of  $\beta$ -catenin/E-cadherin, based on high stringency washes, is much lower than that of  $\beta$ -catenin bound to the complete cytoplasmic domain of E-cadherin. Neither the BB1 domain alone nor  $\beta$ -catenin binding, per se, specifies protein delivery to the basal-lateral membrane.



CD7/CD7BB1 and catenins, respectively. Numbers at the right mark the positions of molecular mass in kD.

**Figure 11.** Catenins bind weakly to CD7BB1. MDCK cells expressing human CD7, or the chimeric protein CD7BB1 were grown on Transwell™ filters for 7 d, labeled for 24 h with  $^{35}\text{S}$ -Met/Cys, extracted with Triton X-100 lysis buffer, and immunoprecipitated with monoclonal antibody T3.3A1 (against the extracellular domain of human CD7). Identical samples were resolved by 7.5% or 10% SDS-PAGE to obtain better separation of

We also expressed a truncated E-cadherin, E-cad8 (Fig. 12), containing the complete extracellular and transmembrane domains, and cytoplasmic domain up to aa 115 (i.e., a deletion of aa 116–151 of the cytoplasmic domain), which is identical to the COOH-terminal deletion in GP2CAD8 (see Fig. 4). This deletion covers the minimal  $\beta$ -catenin binding site (Stappert and Kemler, 1994), and  $\beta$ -catenin is not coimmunoprecipitated in a complex with E-cad8 (data not shown) as reported previously (Stappert and Kemler, 1994). E-cad8 was epitope tagged at its COOH terminus with the KT3 epitope tag, which enabled us to distinguish its distribution in cells expressing endogenous E-cadherin. In confluent monolayers of MDCK cells, in which cell–cell contacts are clear (Fig. 12 B), E-cad8 is not apparent at cell–cell contacts but is localized to intracellular compartments. The staining patterns comprise bright, punctate

structures that are present, although less abundant in cells expressing GP2CAD10 (Fig. 5 B), and a diffuse cytoplasmic staining also similar to that of GP2CAD10 (Fig. 5 B). The extracellular and membrane proximal cytoplasmic domains of cadherin have been proposed to be involved in dimer formation (Shapiro et al., 1995; Nagar et al., 1996; Briehet et al., 1996; Yap et al., 1998). To test whether E-cad8 interacted with endogenous E-cadherin, we separated proteins extracted from MDCK cells expressing E-cad8 using a Superose 6 size exclusion column. Endogenous E-cadherin eluted in fractions 13–16 (Fig. 12 C, see legend for details), as shown previously (Stewart and Nelson, 1997). However, E-cad8 eluted in fractions 16–19 in a profile distinctively different from that of endogenous E-cadherin (Fig. 12 C). Note that E-cad8 has an apparent molecular mass smaller than that of full-length E-cadherin, which is consistent with the cytoplasmic domain deletion. A protein band with an apparent molecular mass greater than that of the full-length E-cadherin probably represents the precursor form of E-cad8 (Ozawa and Kemler, 1990). We also found an enrichment of higher molecular mass precursor forms of three other E-cadherin cytoplasmic domain deletion mutants when expressed in MDCK cells (data not shown).

## Discussion

How membrane proteins are sorted and delivered to different plasma membrane domains in polarized epithelial cells is an important question. However, to date most studies have focused on single proteins that do not form a complex with subunit membrane or cytosolic proteins during their transit through the secretory pathway. Although these studies have identified several types of intrinsic basal-lateral sorting signals in the cytoplasmic domain of a

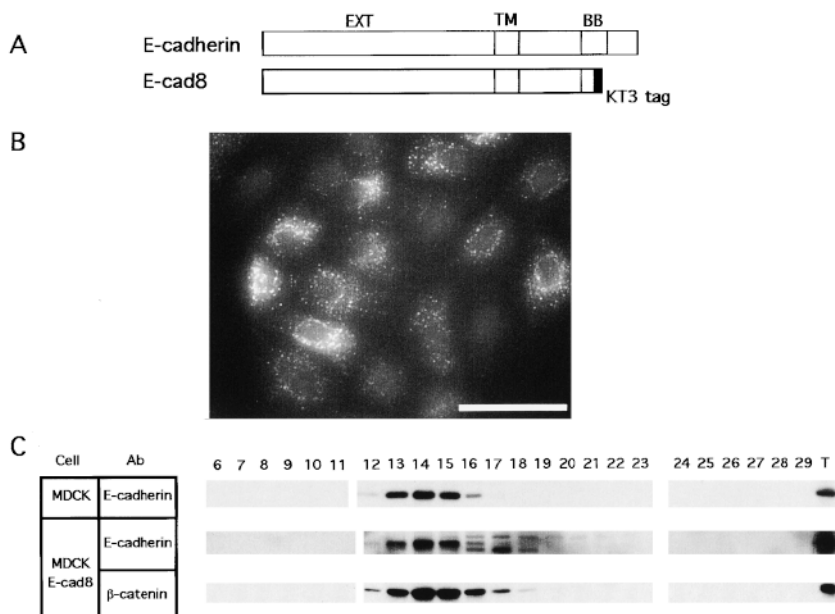


**Figure 12.** Intracellular localization and size exclusion column elution profile of E-cad8 are distinctively different from those of full-length E-cadherin. (A) Schematic diagram of E-cad8 compared with full-length E-cadherin. The COOH-terminal 36 aa of E-cadherin are deleted in E-cad8. This deletion is equivalent to the deletion in GP2CAD8 (Fig. 4). The KT3 epitope tag was fused at the COOH terminus of the cytoplasmic domain of E-cad8. EXT, extracellular domain; TM, transmembrane domain; BB,  $\beta$ -catenin binding domain. Note the diagram is not to scale. (B) Immunofluorescence staining of E-cad8 in MDCK cells using monoclonal antibody KT3. Bar, 50  $\mu\text{m}$ . (C) Elution profile of full-length E-cadherin, E-cad8, and  $\beta$ -catenin after Superose 6 size exclusion chromatography. Individual fractions were resolved by SDS-PAGE and proteins were probed with a monoclonal antibody against the extracellular domain of E-cadherin or a monoclonal antibody against  $\beta$ -catenin. The numbers given on top of the gels are the fraction numbers.

Note that there are three polypeptide bands in the MDCK E-cad8/E-cadherin Western blot. E-cad8 has an electrophoretic mobility faster than that of full-length E-cadherin, which is consistent with the cytoplasmic domain deletion. Full-length E-cadherin is the middle polypeptide band. A protein band with an electrophoretic mobility slower than that of the full-length E-cadherin probably represents the precursor form of E-cad8. T, total cell lysate.

few proteins (Matter and Mellman, 1994), it is not known whether they can be generalized to transmembrane proteins with heterologous binding partners.

E-cadherin is different from other type-I single-span transmembrane protein that have been used to study sorting signals, since it forms a 1:1:1 stoichiometric complex with two cytosolic proteins,  $\beta$ -catenin and  $\alpha$ -catenin (Ozawa and Kemler, 1992). Significantly, previous studies implied that assembly of the E-cadherin/ $\beta$ -catenin complex occurs in the very early stage of trafficking (Ozawa and Kemler, 1992; Hinck et al., 1994a; this study). Therefore, E-cadherin must be sorted to the basal-lateral membrane in a complex with  $\beta$ -catenin. Amino acid sequences in the cytoplasmic domain of E-cadherin that are superficially similar to recently described ER exit (Nishimura and Balch, 1997) and basal-lateral sorting signals (Matter et al., 1992) in other proteins do not have these functions in E-cadherin. Instead, assembly of the E-cadherin/ $\beta$ -catenin complex is the obligatory step in efficient export from the ER, and subsequent delivery of E-cadherin to the basal-lateral membrane of polarized MDCK cells.

### Defining the $\beta$ -Catenin Binding Site in E-Cadherin

To examine domains of E-cadherin important in its sorting to the basal-lateral membrane domain, we used a chimeric protein approach. The chimera was composed of the extracellular domain of GP2, which is normally attached to the membrane through a GPI-anchor, fused to the transmembrane and cytoplasmic domains of E-cadherin (GP2-CAD1). The extracellular domain of GP2, when expressed without a membrane anchor, was secreted equally from both apical and basal-lateral membranes, showing that this domain does not contain specific membrane sorting signals. Using a similar approach, we showed that the extracellular domain of E-cadherin does not contain signals that specify sorting to the basal-lateral membrane. The chimeric protein GP2CAD1, however, was delivered directly to the basal-lateral membrane domain with a rate, efficiency and fidelity similar to that of endogenous E-cadherin.

GP2CAD1 also formed a complex with  $\alpha$ - and  $\beta$ -catenin with a stoichiometry of  $\sim$ 1:1:1 that was resistant to disruption with a high stringency buffer containing 0.1% SDS, 1% deoxycholate and 1 M NaCl, similar to E-cadherin. The design of truncation mutants of GP2CAD1 used to examine sorting signals in the cytoplasmic domain of E-cadherin took into account a previously defined minimal  $\beta$ -catenin binding domain that had been mapped to a region of 30 aa, corresponding to aa 100–129 (Stappert and Kemler, 1994). However, we found that  $\beta$ -catenin did not bind, under these stringent conditions, to a slightly longer region containing this minimal  $\beta$ -catenin binding domain, aa 83–129, if regions of the cytoplasmic domain around it had been deleted (e.g., GP2CAD5, 7, 9, and 10).

We tested whether this difference between our results and those of Stappert and Kemler (1994) reflected the difference in the cell types used to express these mutants (L cells, MDCK cells). GP2CAD1, 6, 7, 8, and 10 were transiently transfected into L cells and HEK293 cells. By immunofluorescence in both cell types, GP2CAD1 was localized to the cell surface, whereas GP2CAD6, 7, 8, and 10

were predominantly localized to the ER (Y.-T. Chen, unpublished results), similar to their locations in MDCK cells (summarized in Fig. 4). Another reason for the difference in results might be the methods used to assess the stoichiometry of  $\beta$ -catenin binding to this minimal binding site on E-cadherin. However, Stappert and Kemler (1994), did not quantitate the stoichiometry of the complex formed between  $\beta$ -catenin and the minimal  $\beta$ -catenin binding domain (aa 100–129). We found that  $\beta$ -catenin bound to a chimeric protein composed of CD7 and aa 83–129 of the E-cadherin cytoplasmic domain (CD7BB1), but the stoichiometry of the coimmunoprecipitated complex was  $\sim$ 5:1 after a high stringency wash. Recently, Finnemann et al. (1997) reported the expression of three COOH-terminal deletion mutants of *Xenopus* XB/U-cadherin in L cells. A deletion of the most COOH-terminal 19 amino acids, which would contain the minimal  $\beta$ -catenin binding domain intact, bound  $\beta$ -catenin but the adhesion function of the truncated cadherin was interpreted to be “dramatically altered.” We note that biochemical data presented in the same paper (Fig. 3 in Finnemann et al., 1997) revealed a decrease in the avidity of  $\beta$ -catenin binding to the mutant cadherin. Interestingly, confocal microscopy of L cells expressing XB/U-cadherin revealed that full-length protein localized to cell–cell contacts, whereas the truncation mutant had a distinctly different location and appeared to have a punctate distribution. In conclusion, it seems likely that  $\beta$ -catenin binds to a minimal domain of E-cadherin comprising aa 100–129, but the interaction is considerably weaker than binding of  $\beta$ -catenin to the whole cytoplasmic domain of E-cadherin. Reduced binding of the cytoplasmic domain of cadherin to  $\beta$ -catenin leads to intracellular retention and reduced cell surface expression of cadherin.

The cadherin-binding domain in  $\beta$ -catenin lies within the armadillo (arm) repeats of  $\beta$ -catenin (Hulsken et al., 1994). The crystal structure of the arm repeats revealed a rigid cylindrical super-helix of helices that form a groove lined with positively-charged amino acids (Huber et al., 1997). The length of this groove could potentially accommodate a fully extended peptide of aa 25–30, or a longer peptide with local secondary structures; note that the minimal  $\beta$ -catenin binding site on E-cadherin is 29 aa and has a pI of 3.1 (see Huber et al., 1997). Although structural analysis of the E-cadherin/ $\beta$ -catenin cocrystal is required to define the interaction in detail, our recent analysis has revealed that the cytoplasmic domain of E-cadherin is protected from proteolysis when it has formed a 1:1 stoichiometric complex with the  $\beta$ -catenin arm repeats (Huber, A., D.B. Stewart, W.J. Nelson, and W. Weis, in preparation). This result is compatible with the view formed from the present studies of  $\beta$ -catenin binding to GP2CAD1 deletion mutants in which most of the cytoplasmic domain of E-cadherin, including the previously mapped minimal  $\beta$ -catenin binding domain, interacts with  $\beta$ -catenin.

### $\beta$ -Catenin/E-Cadherin Binding Is Coupled to Efficient Exit of E-Cadherin from the ER

Using a combination of results obtained by cell surface biotinylation, sensitivity to endoglycosidase H digestion, immunoprecipitation, and immunofluorescence we have shown that GP2CAD1 bound  $\beta$ -catenin and >90% en-

tered the secretory pathway to the basal-lateral membrane. However, GP2CAD1 deletion mutants did not bind  $\alpha$ - or  $\beta$ -catenin and >90% remained in the ER. Previous studies indicated that newly synthesized E-cadherin binds  $\beta$ -catenin soon after its synthesis, and that  $\alpha$ -catenin binds to the complex when E-cadherin arrives at the cell surface (Ozawa and Kemler, 1992; Hinck et al., 1994a). Thus, formation of the E-cadherin/ $\beta$ -catenin complex correlates with efficient exit of E-cadherin from the ER.

It is possible that E-cadherin has a specific ER export signal that is deleted from the GP2CAD1 mutants. Recently, it was reported that the COOH-terminal acidic residues of VSV-G protein are involved in efficient exit of VSV-G protein from ER (Nishimura and Balch, 1997), and that deletion of the most COOH-terminal two valine residues of proTGF $\alpha$  resulted in the ER accumulation of the protein (Briley et al., 1997). It has been suggested that COOH-terminal acidic amino acid residues constitute an ER export signal (Nishimura and Balch, 1997). In this regard, it is striking that our results showed that a deletion of the COOH-terminal three acidic amino acids of GP2CAD1 resulted in the accumulation of the protein (GP2CAD10) in the ER. However, our data are not consistent with the possibility that these, or other acidic amino acids at the COOH terminus constitute a minimal ER exit signal. Internal deletions of the cytoplasmic domain of E-cadherin (e.g., GP2CAD3) resulted in retention of the protein in the ER, even though COOH-terminal acidic amino acids were intact. In general, we cannot separate the roles of different regions/motifs as ER export signals from the dominant requirement for high affinity binding of  $\beta$ -catenin to the whole cytoplasmic domain of E-cadherin. It seems more likely that the complex of E-cadherin/ $\beta$ -catenin presents a conformation or motif in the cytoplasmic domain of E-cadherin that allows efficient export of the complex from the ER. Definitive proof of this mechanism will require the expression of E-cadherin in a cell line lacking both  $\beta$ -catenin and plakoglobin. ER retention of GP2CAD1 proteins containing a truncated cytoplasmic domain is likely to be a consequence of missfolding, due to inhibition of  $\beta$ -catenin binding (see Fig. 9). These misfolded proteins are targeted subsequently for degradation in either lysosomes or the 26S proteasome (Fig. 8). Finally, our analysis of the distribution of the simple deletion mutant E-cad8 (Fig. 12), which was not a chimeric protein, showed that this mutant was also localized intracellularly. E-cad8 did not form a complex with endogenous E-cadherin despite an intact extracellular and membrane proximal cytoplasmic domain, which have been identified as potential sites for dimer formation (Shapiro et al., 1995; Nagar et al., 1996; Briehner et al., 1996; Yap et al., 1998). Thus, E-cadherin dimerization may not occur in the absence of  $\beta$ -catenin binding, or is dependent on E-cadherin leaving the ER or arriving at the plasma membrane.

### ***$\beta$ -Catenin Binding to E-Cadherin and Delivery of E-Cadherin to Sites of Function in the Basal-lateral Membrane Domain of the Cell Surface***

Previous studies have emphasized that sorting of transmembrane proteins to either the apical or basal-lateral membrane occurs in the TGN (Matter and Mellman,

1994). For example, early studies showed that influenza virus HA and VSV-G protein appeared together in vesicles and membrane compartments until the TGN where they appeared to be segregated into separate vesicle populations (Fuller et al., 1985). Our data show that complex formation between E-cadherin cytoplasmic domain and  $\beta$ -catenin in the ER is not only coupled to efficient export of E-cadherin but also direct delivery of E-cadherin to the basal-lateral membrane. Note that in the absence of complex formation with  $\beta$ -catenin, a small amount (<10%) of GP2CAD1 deletion mutants leaked out of the ER and were then delivered randomly to both the apical and basal-lateral membranes. As in the case of ER export, we suggest that binding of  $\beta$ -catenin to E-cadherin induces a conformation state in the cytoplasmic domain of E-cadherin that reveals a sorting determinant(s) that is recognized by the basal-lateral sorting machinery. Thus,  $\beta$ -catenin may function as a chauffeur to facilitate E-cadherin transport through the secretory pathway. At present, we cannot rule out an alternative possibility that  $\beta$ -catenin itself contains basal-lateral membrane targeting information, and that this information is recognized by the sorting machinery for delivery of the E-cadherin/ $\beta$ -catenin complex to the basal-lateral membrane.

That binding of  $\beta$ -catenin to the cytoplasmic domain of E-cadherin plays an essential role in the efficient delivery of E-cadherin to the cell surface raises the interesting possibility that ER exit is a potential regulatory point for E-cadherin function. For example, limited availability of  $\beta$ -catenin for binding to E-cadherin, or post-translational modifications to  $\beta$ -catenin that reduce the affinity of E-cadherin/ $\beta$ -catenin binding might lead to the retention of un-complexed E-cadherin in the ER. Since the half-life of E-cadherin is quite short (<5 h in MDCK cells; Shore and Nelson, 1991), retention of newly synthesized E-cadherin in the ER would quickly result in reduced cell surface expression of E-cadherin and, consequently, reduced cell-cell adhesion. We note that  $\beta$ -catenin is a component of the Wnt/Wingless signaling pathway in which regulation of  $\beta$ -catenin levels is critical (Cadigan and Nusse, 1997). Significantly, there is evidence that changes in  $\beta$ -catenin levels leads to changes in steady state and cell surface levels of cadherins, and increased cadherin-mediated cell-cell adhesion (Bradley et al., 1993; Hinck et al., 1994b; Yanagawa et al., 1997). These effects on cadherin could be mediated by the availability of  $\beta$ -catenin for binding to cadherin in the ER, which regulates cadherin entry into the secretory pathway and, therefore, the amount of cadherin available for adhesion functions at the cell surface.

We thank Dr. Anson Lowe for providing cDNA clone of rat GP2 and anti-GP2 antibody, Dr. Gernot Walter for KT3 antibody, Dr. Brian Seed for human CD7 cDNA clone.

This work was supported by grants to W.J. Nelson from the National Institutes of Health. Y.-T. Chen is a recipient of a postdoctoral fellowship from the National Kidney Foundation (NKF), and D.B. Stewart is the recipient of a pre-doctoral fellowship from the Howard Hughes Medical Institute.

Received for publication 13 February 1998 and in revised form 13 January 1999.

### ***References***

Aberle, H., S. Butz, J. Stappert, H. Weissig, R. Kemler, and H. Hoschuetzky.

1994. Assembly of the cadherin-catenin complex in vitro with recombinant proteins. *J. Cell Sci.* 107:3655–3663.
- Aruffo, A., and B. Seed. 1987a. Molecular cloning of a CD28 cDNA by a high-efficiency COS cell expression system. *Proc. Natl. Acad. Sci. USA.* 84:8573–8577.
- Aruffo, A., and B. Seed. 1987b. Molecular cloning of two CD7 (T-cell leukemia antigen) cDNAs by a COS cell expression system. *EMBO (Eur. Mol. Biol. Organ.) J.* 6:3313–3331.
- Bradley, R.S., P. Cowin, and A.M. Brown. 1993. Expression of Wnt-1 in PC12 cells results in modulation of plakoglobin and E-cadherin and increased cellular adhesion. *J. Cell Biol.* 123:1857–1865.
- Briehner, W.M., A.S. Yap, and B.M. Gumbiner. 1996. Lateral dimerization is required for the homophilic binding activity of C-cadherin. *J. Cell Biol.* 135:487–496.
- Briley, G.P., M.A. Hissong, M.L. Chiu, and D.C. Lee. 1997. The carboxyl-terminal valine residues of proTGF alpha are required for its efficient maturation and intracellular routing. *Mol. Biol. Cell.* 8:1619–1631.
- Brown, D.A., B. Crise, and J.K. Rose. 1989. Mechanism of membrane anchoring affects polarized expression of two proteins in MDCK cells. *Science.* 245:1499–1501.
- Bush, K.T., A.L. Goldberg, and S.K. Nigam. 1997. Proteasome inhibition leads to a heat-shock response, induction of endoplasmic reticulum chaperones, and thermotolerance. *J. Biol. Chem.* 272:9086–9092.
- Cadigan, K.M., and R. Nusse. 1997. Wnt signaling: a common theme in animal development. *Genes Dev.* 11:3286–3305.
- Casanova, J.E., G. Apodaca, and K.E. Mostov. 1991. An autonomous signal for basolateral sorting in the cytoplasmic domain of the polymeric immunoglobulin receptor. *Cell.* 66:65–75.
- Chen, Y.-T., C. Holcomb, and H.P. Moore. 1993. Expression and localization of two low molecular weight GTP-binding proteins, Rab8 and Rab10, by epitope tag. *Proc. Natl. Acad. Sci. USA.* 90:6508–6512.
- Coux, O., K. Tanaka, and A.L. Goldberg. 1996. Structure and functions of the 20S and 26S proteasomes. *Annu. Rev. Biochem.* 65:801–847.
- Finnemann, S., I. Mitrik, M. Hess, G. Otto, and D. Wedlich. 1997. Uncoupling of XB/U-cadherin-catenin complex formation from its function in cell-cell adhesion. *J. Biol. Chem.* 272:11856–11862.
- Fuller, S.D., R. Bravo, and K. Simons. 1985. An enzymatic assay reveals that proteins destined for the apical or basolateral domains of an epithelial cell line share the same late Golgi compartments. *EMBO (Eur. Mol. Biol. Organ.) J.* 4:297–307.
- Graeve, L., A. Patzak, K. Drickamer, and E. Rodriguez-Boulan. 1990. Polarized expression of functional rat liver asialoglycoprotein receptor in transfected Madin-Darby canine kidney cells. *J. Biol. Chem.* 265:1216–1224.
- Hammerton, R.W., K.A. Krzeminski, R.W. Mays, T.A. Ryan, D.A. Wollner, and W.J. Nelson. 1991. Mechanism for regulating cell surface distribution of Na(+)/K(+)-ATPase in polarized epithelial cells. *Science.* 254:847–850.
- Hinck, L., I.S. Nathke, J. Papkoff, and W.J. Nelson. 1994a. Dynamics of cadherin/catenin complex formation: novel protein interactions and pathways of complex assembly. *J. Cell Biol.* 125:1327–1340.
- Hinck, L., W.J. Nelson, and J. Papkoff. 1994b. Wnt-1 modulates cell-cell adhesion in mammalian cells by stabilizing beta-catenin binding to the cell adhesion protein cadherin. *J. Cell Biol.* 124:729–741.
- Hoops, T.C., and M.J. Rindler. 1991. Isolation of the cDNA encoding glycoprotein-2 (GP-2), the major zymogen granule membrane protein. Homology to uromodulin/Tamm-Horsfall protein. *J. Biol. Chem.* 266:4257–4263.
- Huber, A.H., W.J. Nelson, and W.I. Weis. 1997. Three-dimensional structure of the armadillo repeat region of beta-catenin. *Cell.* 90:871–882.
- Hulsken, J., W. Birchmeier, and J. Behrens. 1994. E-cadherin and APC compete for the interaction with beta-catenin and the cytoskeleton. *J. Cell Biol.* 127:2061–2069.
- Hunziker, W., and C. Fumey. 1994. A di-leucine motif mediates endocytosis and basolateral sorting of macrophage IgG Fc receptors in MDCK cells. *EMBO (Eur. Mol. Biol. Organ.) J.* 13:2963–2967.
- Jou, T.S., D.B. Stewart, J. Stappert, W.J. Nelson, and J.A. Marrs. 1995. Genetic and biochemical dissection of protein linkages in the cadherin-catenin complex. *Proc. Natl. Acad. Sci. USA.* 92:5067–5071.
- Kemler, R. 1992. Classical cadherins. *Semin. Cell Biol.* 3:149–155.
- Knudsen, K.A., A.P. Soler, K.R. Johnson, and M.J. Wheelock. 1995. Interaction of alpha-actinin with the cadherin/catenin cell-cell adhesion complex via alpha-catenin. *J. Cell Biol.* 130:67–77.
- Le Bivic, A., Y. Sambuy, K. Mostov, and E. Rodriguez-Boulan. 1990. Vectorial targeting of an endogenous apical membrane asialoglycoprotein and uromodulin in MDCK cells. *J. Cell Biol.* 110:1533–1539.
- Lisanti, M.P., I.W. Caras, M.A. Davitz, and E. Rodriguez-Boulan. 1989. A glycopospholipid membrane anchor acts as an apical targeting signal in polarized epithelial cells. *J. Cell Biol.* 109:2145–2156.
- MacArthur, H., and G. Walter. 1984. Monoclonal antibodies specific for the carboxy terminus of simian virus 40 large T antigen. *J. Virol.* 52:483–491.
- Marrs, J.A., E.W. Napolitano, C. Murphy-Erdosh, R.W. Mays, L.F. Reichardt, and W.J. Nelson. 1993. Distinguishing roles of the membrane-cytoskeleton and cadherin mediated cell-cell adhesion in generating different Na(+)/K(+)-ATPase distributions in polarized epithelia. *J. Cell Biol.* 123:149–164.
- Matter, K., W. Hunziker, and I. Mellman. 1992. Basolateral sorting of LDL receptor in MDCK cells: the cytoplasmic domain contains two tyrosine-dependent targeting determinants. *Cell.* 71:741–753.
- Matter, K., and I. Mellman. 1994. Mechanisms of cell polarity: sorting and transport in epithelial cells. *Curr. Opin. Cell Biol.* 6:545–554.
- Matter, K., E.M. Yamamoto, and I. Mellman. 1994. Structural requirements and sequence motifs for polarized sorting and endocytosis of LDL and Fc receptors in MDCK cells. *J. Cell Biol.* 126:991–1004.
- Mays, R.W., K.A. Siemers, B.A. Fritz, A.W. Lowe, G. van Meer, and W.J. Nelson. 1995. Hierarchy of mechanisms involved in generating Na/K-ATPase polarity in MDCK epithelial cells. *J. Cell Biol.* 130:1105–1115.
- Nagafuchi, A., and M. Takeichi. 1988. Cell binding function of E-cadherin is regulated by the cytoplasmic domain. *EMBO (Eur. Mol. Biol. Organ.) J.* 7:3679–3684.
- Nagafuchi, A., Y. Shirayoshi, K. Okazaki, K. Yasuda, and M. Takeichi. 1987. Transformation of cell adhesion properties by exogenously introduced E-cadherin cDNA. *Nature.* 329:341–343.
- Nagar, B., M. Overduin, M. Ikura, and J.M. Rini. 1996. Structural basis of calcium-induced E-cadherin rigidification and dimerization. *Nature.* 380:360–364.
- Nelson, W.J. 1992. Regulation of cell surface polarity from bacteria to mammals. *Science.* 258:948–955.
- Nishimura, N., and W.E. Balch. 1997. A di-acidic signal required for selective export from the endoplasmic reticulum. *Science.* 277:556–558.
- Nosjean, O., A. Briolay, and B. Roux. 1997. Mammalian GPI proteins: sorting, membrane residence and functions. *Biochim. Biophys. Acta.* 1331:153–186.
- Ozawa, M., and R. Kemler. 1990. Correct proteolytic cleavage is required for the cell adhesive function of uromodulin. *J. Cell Biol.* 111:1645–1650.
- Ozawa, M., and R. Kemler. 1992. Molecular organization of the uromodulin-catenin complex. *J. Cell Biol.* 116:989–996.
- Ozawa, M., M. Ringwald, and R. Kemler. 1990. Uromodulin-catenin complex formation is regulated by a specific domain in the cytoplasmic region of the cell adhesion molecule. *Proc. Natl. Acad. Sci. USA.* 87:4246–4250.
- Pagano, R.E., M.A. Sepanski, and O.C. Martin. 1989. Molecular trapping of a fluorescent ceramide analogue at the Golgi apparatus of fixed cells: interaction with endogenous lipids provides a trans-Golgi marker for both light and electron microscopy. *J. Cell Biol.* 109:2067–2079.
- Palmgren, M.G. 1991. Acridine orange as a probe for measuring pH gradients across membranes: mechanism and limitations. *Anal Biochem.* 192:316–321.
- Rimm, D.L., E.R. Koslov, P. Kebriaei, C.D. Cianci, and J.S. Morrow. 1995. Alpha 1(E)-catenin is an actin-binding and -bundling protein mediating the attachment of F-actin to the membrane adhesion complex. *Proc. Natl. Acad. Sci. USA.* 92:8813–8817.
- Rodriguez-Boulan, E., and W.J. Nelson. 1989. Morphogenesis of the polarized epithelial cell phenotype. *Science.* 245:718–725.
- Rodriguez-Boulan, E., and S.K. Powell. 1992. Polarity of epithelial and neuronal cells. *Annu. Rev. Cell Biol.* 8:395–427.
- Shapiro, L., A.M. Fannon, P.D. Kwong, A. Thompson, M.S. Lehmann, G. Grubel, J.F. Legrand, J. Als-Nielsen, D.R. Colman, and W.A. Hendrickson. 1995. Structural basis of cell-cell adhesion by cadherins. *Nature.* 374:327–337.
- Shore, E.M., and W.J. Nelson. 1991. Biosynthesis of the cell adhesion molecule uromodulin (E-cadherin) in Madin-Darby canine kidney epithelial cells. *J. Biol. Chem.* 266:19672–19680.
- Simons, K., and N.A. Wandering. 1990. Polarized sorting in epithelia. *Cell.* 62:207–210.
- Southern, P.J., and P. Berg. 1982. Transformation of mammalian cells to antibiotic resistance with a bacterial gene under control of the SV40 early region promoter. *J. Mol. Appl. Genet.* 1:327–341.
- Stappert, J., and R. Kemler. 1994. A short core region of E-cadherin is essential for catenin binding and is highly phosphorylated. *Cell Adhes. Commun.* 2:319–327.
- Stewart, D.B., and W.J. Nelson. 1997. Identification of four distinct pools of catenins in mammalian cells and transformation-dependent changes in catenin distributions between these pools. *J. Biol. Chem.* 272:29652–29662.
- Thomas, D.C., C.B. Brewer, and M.G. Roth. 1993. Vesicular stomatitis virus glycoprotein contains a dominant cytoplasmic basolateral sorting signal critically dependent upon a tyrosine. *J. Biol. Chem.* 268:3313–3320.
- Weimbs, T., S.-H. Low, S.J. Chapin, and K.E. Mostov. 1997. Apical targeting in polarized epithelial cells. *Trends Cell Biol.* 7:393–399.
- Yanagawa, S.I., J.S. Lee, T. Haruna, H. Oda, T. Uemura, M. Takeichi, and A. Ishimoto. 1997. Accumulation of Armadillo induced by Wingless, Dishevelled, and dominant-negative Zeste-White 3 leads to elevated DE-cadherin in *Drosophila* clone 8 wing disc cells. *J. Biol. Chem.* 272:25243–25251.
- Yap, A.S., C.M. Niessen, and B.M. Gumbiner. 1998. The juxtamembrane region of the cadherin cytoplasmic tail supports lateral clustering, adhesive strengthening, and interaction with p120ctn. *J. Cell Biol.* 141:779–789.